Available online at www.sciencedirect.com
ScienceDirect
Journal of the European Ceramic Society 31 (2011) 175–181
www.elsevier.com/locate/jeurceramsoc

Liquid phase formation in the system SiC, Al_2O_3, Y_2O_3

R. Neher[a,*], M. Herrmann[a], K. Brandt[a], K. Jaenicke-Roessler[a], Z. Pan[b], O. Fabrichnaya[b], H.J. Seifert[b]

[a] *Fraunhofer Institut für keramische Technologien and Systeme, 01277 Dresden, Germany*
[b] *Institut für Werkstoffwissenschaft der TU Bergakademie Freiberg, 09599 Freiberg, Germany*

Received 26 May 2010; received in revised form 20 August 2010; accepted 4 September 2010

Abstract

The liquid phase formation in the system SiC–Al_2O_3–Y_2O_3 was investigated via differential thermal analysis (DTA) combined with thermogravimetry (TG). For this purpose mixtures of various alumina and yttria mol ratios and 10 and 20 mol% silicon carbide were densified and heat treated at different temperatures. It was shown that silicon carbide in the examined amounts has low influence on the melting temperature of the oxide phase. The compositions and microstructures formed were studied by SEM, EDX and XRD. The results were compared to thermodynamic calculations.

Keywords: SiC; Al_2O_3; Y_2O_3; Sintering; SPS/FAST

1. Introduction

Silicon carbide (SiC) is the most deployed non-oxide ceramic in the world.[1] Its high temperature stability, the high hardness and the excellent resistance against oxidation and corrosion are some of the advantages of silicon carbide ceramics in technical applications.

The classical way of solid phase sintering of SiC (SSiC) is performed at high temperatures up to 2200 °C where additions of small amounts of boron, aluminium and carbon make the production of dense SiC technically manageable.[2,3] SiC arising from this process is quasi single phase with all the above mentioned properties. Alternative sintering methods have been developed to lower the sintering temperatures and to improve fracture toughness and mechanical strength. The use of rare earths together with alumina and AlN, respectively, allows a liquid phase sintering (LPS) of SiC.[4] These additives form a liquid phase at temperatures above 1850 °C allowing the reduction of the sintering temperature. During cooling the liquid phase solidifies to crystallised phases such as rare earth aluminates or oxynitrides (in the case of AlN). These additives strongly change the mechanical properties of the material in comparison to the solid phase sintered ceramics. An increase of fracture toughness up to 100% and an increase of flexural strength up to 70% in comparison to SSiC can be achieved.[2] Also the electrical properties[5] and the chemical resistance[6] are influenced.

Thus for the liquid phase sintering of SiC the phase relations in the SiC–Al_2O_3–Y_2O_3 system and melting temperatures at different ratio of components are of interest. The publications addressing this system are rare and mostly deal with the interaction of the oxides and SiC with the sintering atmosphere.[7–9] No reliable data exist concerning the composition of the liquid phase and the eutectic or peritectic temperatures. The observed liquid phase sintering mechanism requires some dissolution of SiC in the liquid phase. The observed incorporation of small amounts of alumina into the SiC grains and the fast phase transformation from β- to α-SiC during liquid phase sintering are evidences of such a solution. In work of Hoffmann and Nader[10] it was estimated, that the solubility of the SiC at sintering temperatures should be in the range of 10 mass%. However no experimental data concerning the solubility and the liquidus formation in the system SiC–Al_2O_3–Y_2O_3 exists. Therefore, the aim of present work is a detailed investigation of phase equilibria in the system SiC–Al_2O_3–Y_2O_3 including melting behaviour.

The liquid phase formation in the system SiC–Al_2O_3–Y_2O_3 was investigated by simultaneous thermal analysis (STA), ceramographic and XRD methods. Additionally the experimental

* Corresponding author. Tel.: +49 351 2553 7713; fax: +49 351 2554 227.
E-mail address: roland.neher@ikts.fraunhofer.de (R. Neher).

0955-2219/$ – see front matter © 2010 Elsevier Ltd. All rights reserved.
doi:10.1016/j.jeurceramsoc.2010.09.002

Table 1
Samples and corresponding compositions.

Sample	SiC [mol%]	Mol ratio Y_2O_3/Al_2O_3
YAlSiC-		
208000	0	20/80
208010	10	20/80
208020	20	20/80
YAlSiC-		
455500	0	45/55
455510	10	45/55
455520	20	45/55
YAlSiC-		
604000	0	60/40
604010	10	60/40
604020	20	60/40
YAlSiC-		
802000	0	80/20
802010	10	80/20
802050	50	80/20

data of this paper are compared with thermodynamic calculations of the quasi-ternary system $SiC–Al_2O_3–Y_2O_3$.[11]

2. Experimental

Specimen with silicon carbide contents of 10 mol%, 20 mol% and one with 50 mol% were produced (Table 1 and Fig. 1). The high oxide content leads to significant effects in the DTA and also the solubility of SiC in the liquid melt is assumed to be less than 10 mass%[10]. High SiC contents are assumed to have no effect on melting temperatures. Compositions without silicon carbide were additionally prepared to be able to compare the results to literature data and to study the effect of the SiC on the melting temperatures. The ratio of yttria/alumina was changed from 20/80 over 45/55 and 60/40 to 80/20, according to the eutectic- (and one intermediate, 60/40) compositions in the pseudo binary phase diagram $Al_2O_3–Y_2O_3$. All specimen and their corresponding compositions are shown in Table 1. The powders used to produce the mixtures were SiC (grade UF15, H.C. Starck Germany, oxygen concentration < 1.5%), α-Al_2O_3 (AKP 50, Sumitomo Chemical Co.) and Y_2O_3 (grade C, H.C. Starck Germany). The powders were mixed in isopropanol in a planetary ball mill (200 rpm, 2 h) and then dried in a rotary evaporator. Afterwards the silicon carbide containing powders were densified via spark plasma sintering (SPS, device: HP D 25/1 of FCT Systeme GmbH) for 5 min at 1400 °C in vacuum with a pressure of 50 MPa. The heating rate was 100 K/min. As a result the materials were compacted to dense samples with 40 mm diameter and 5 mm height. The achievement of full density at low temperatures ensures a strong reduction of the decomposition of the materials taking place at higher temperatures due to the interaction with the atmospheres (see e.g. [8]). These samples were the basis for all further heat treatments and the DTA/TG analysis.

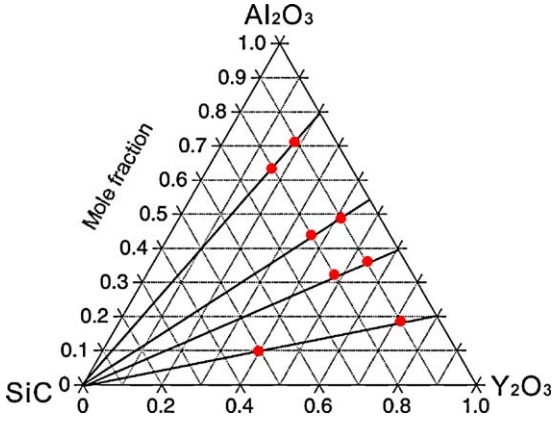

Fig. 1. Ternary system $SiC–Y_2O_3–Al_2O_3$. Lines assign the mol ratios yttria to alumina (20/80, 45/55, 60/40 and 80/20). Points mark the compositions of samples produced.

In order to check if the fast SPS process produces equilibrium phases an additional heat treatment of the materials containing 20 mol% SiC was carried out for 1 h at 1700 °C in Argon. This is below the expected melting temperatures. The experiments were done in a graphite heated furnace having the samples embedded in powder mixtures of the same composition as the samples to reduce reactions with atmosphere. In addition the silicon carbide containing samples were molten to reveal the phases and the microstructure after melting and solidification. This was necessary because the DTA samples had a mass of only some mg. The melting was carried out in a graphite heated furnace (Thermal Technologies GmbH) at 1850 °C for samples YAlSiC-2080x and at 1950 °C for samples YAlSiC-4555x, -6040x, -8020x for 5 min in preconditioned graphite crucibles. The heating and cooling rate was 20 K/min and the atmosphere was a mixture of Argon and CO. The preconditioning was done to minimise reactions of specimen with the graphite crucible in the subsequent experiment. For this conditioning the crucibles were filled with powder mixtures of the same composition as the samples and were heat treated in a graphite heated furnace up to 1950 °C in Argon atmosphere.

The powders without silicon carbide were heat treated in a muffle furnace up to 1400 °C in air with a dwelling time of 3 h. Here also the contained phases were checked. It was in agreement with the phases expected by the phase diagram. The heat treatment in air was used, because no decomposition of the materials is expected. In contrast the interaction with the graphite during SPS could change the composition slightly (formation of some carbides or formation of carbon inclusions).

Melting temperatures were determined using differential thermal analysis (DTA) combined with thermogravimetry (TG), also known as simultaneous thermal analysis (STA). Measurements were carried out in the device STA 429 of Netzsch Gerätebau GmbH Selb under static helium atmosphere with heating and cooling rates of 20 K/min in tungsten crucibles using no reference substance. A tungsten heating element and a thermocouple of WRe (3%) and WRe (25%) were used. The temperature was calibrated by the melting points of alumina (NIST SRM 742) and sampling was done from the bulk of the densified samples. The absolute uncertainty of measurement is estimated to be 16 K and the relative one to be 5 K. Since the specimen showed a mass loss when melting began, the maximum heating temperatures were set to a few degrees above the melting temperature.

Table 2
Phases identified by XRD measurements of the materials after densification with the SPS at 1400 °C and after heat treatments at 1700 °C in graphite furnace. And comparison to phases expected by thermodynamical calculations (YAG – $Al_5Y_3O_{12}$, YAP – $AlYO_3$, YAM – $Al_2Y_4O_9$).

		[Mass%]						
Sample		SiC	Al_2O_3	YAG	YAP	YAM	Y_2O_3	Al_4SiC_4
YAlSiC-208010	SPS	3.8	38.6	57.7				
	Thermodyn. calc.	3.4	36.3	60.3				
YAlSiC-208020	SPS	9	36.0	55.1				
	1700 °C	7.9	36.3	55.8				
	Thermodyn. calc.	7.3	34.8	57.9				
YAlSiC-455510	SPS	2.5		35.4	57.2	4.9		
	Thermodyn. calc.	2.7		36.6	60.6			
YAlSiC-455520	SPS	6.5		35	53	5.3		
	1700 °C	6.6		52.6	35.2	5.4		
	Thermodyn. calc.	6.0		35.4	58.6			
YAlSiC-604010	SPS	1.9			42.5	55.7		
	Thermodyn. calc.	2.2			35.7	61.8		0.34
YAlSiC-604020	SPS	4.6			43.0	52.4		
	1700 °C	5.7			42.6	51.7		
	Thermodyn. calc.	5.1			34.6	59.8		0.33
YAlSiC-802010	SPS	3.5				52.6	44.0	
	Thermodyn. calc.	2.0				53.5	44.3	0.25
YAlSiC-802050	SPS	15.7				50.2	34.1	
	Thermodyn. calc.	16.4				45.6	37.7	0.21

The phases occurring in the samples after the different thermal treatments were determined by X-ray diffraction (XRD 7, Seifert FPM, CuKα 10–90° 2Θ). The quantitative analysis was carried out using Rietveld method (Autoquan, GE Inspection Technology). The *R* values of the calculations were in the range of 5–7%. Afterwards the structure and composition of selected samples was examined by FESEM (device: LEO 982 of Carl Zeiss SMT) and EDX (device: Oxford Instruments).

2.1. Thermodynamic modelling

The thermodynamic database derived by Cupid et al.[9] combining description of Fabrichnaya et al.[12] with data of Gröbner[13] was modified to calculate phase relations in the Si–C–Y–Al–O system. A detailed description of this modified database is given by Pan et al.[11]. All thermodynamic calculations of this work use this description. Calculations were performed by THERMO-CALC computer program.[14]

3. Results and discussion

3.1. Subsolidus compositions

From liquid phase sintering experiments[15–18] it can be concluded that Al_2O_3 and the yttria–aluminates have to be in equilibrium with SiC. Therefore the observed formation of the different aluminates and SiC in the subsolidus area after the SPS was expected. The low sintering time in the SPS reduces the interaction with the graphite die and thus a shift of the composition of the materials was not expected. The results of the XRD-measurements after SPS and after heat treatment at 1700 °C in comparison with the calculated phase equilibrium using thermodynamic database is shown in Table 2. The results show, that the phases are formed in amounts, which would be expected under equilibrium conditions. An exception is the sample group YAlSiC-4555x, which is not completely in equilibrium. The monoclinic phase (YAM, $Al_2Y_4O_9$) was detected. Probably this phase has not been entirely converted to the equilibrium phases with garnet (YAG, $Al_5Y_3O_{12}$) and perovskite (YAP, $AlYO_3$) during the SPS.

A careful EDX analysis of the microstructure of the SPS- and heat treated samples does not result in the observation of some SiO_2 containing glasses or crystalline phases. This was to be expected, because the SiO_2 content introduced by silicon carbide is less than 0.15 wt% for the samples with up to 20 mol% SiC. From earlier experiments it is known, that during the SPS SiO_2 is

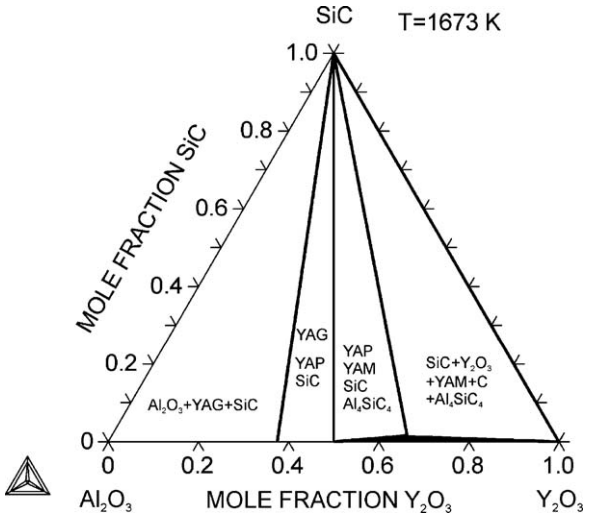

Fig. 2. Phase relation in the ternary system SiC–Al_2O_3–Y_2O_3 at 1400 °C calculated in present study.

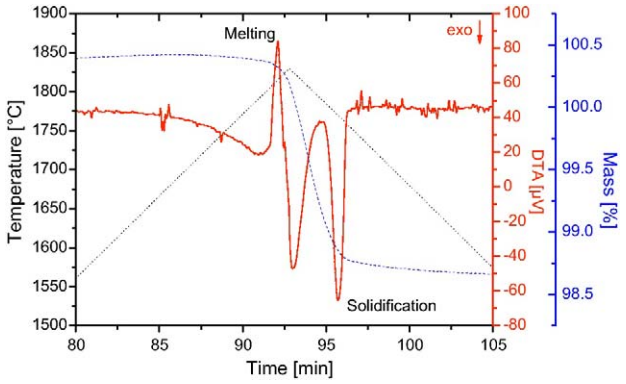

Fig. 3. Result of STA-measurement of YAlSiC-208010 against time. Continuous line shows the DTA-signal, the dashed one the mass change and the dotted one the temperature.

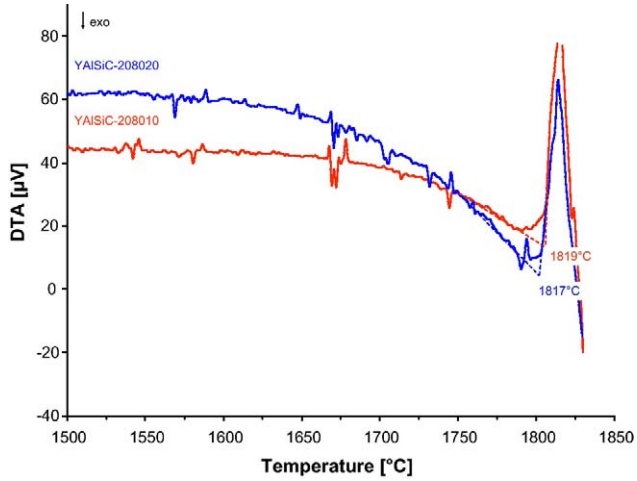

Fig. 4. Detail of STA-measurement of YAlSiC-208010 and YAlSiC-208020 against temperature. Extrapolated onsets of DTA-peaks mark the melting at 1819 °C (YAlSiC-208010) and 1817 °C (YAlSiC-208020).

even partially reduced to SiC. Therefore a remarkable influence on the phase composition and the DTA/TG investigation was not expected.

The small amount of Al_4SiC_4 (<0.25 wt%) indicated by calculations for samples YAlSiC-604010, YAlSiC-604020, YAlSiC-802010 and YAlSiC-802050 was not detected. The reason for these small deviations is reaction of SiC with YAM and Al_2O_3 accompanied by formation of the Al_4SiC_4 phase and dissolution of the SiO_2 in YAM in calculations. The calculated phase diagram of the SiC–Al_2O_3–Y_2O_3 system at 1400 °C is presented in Fig. 2.

3.2. Simultaneous thermal analysis and resulting phase composition

Fig. 3 shows the result of the STA-measurement of sample YAlSiC-208010. Lines are smoothed and Buoyancy effect is not corrected. At heating-up the DTA-signal shows an exothermal decline followed by an endothermal peak. At cooling an exothermal peak occurs. The TG-signal shows one mass loss step.

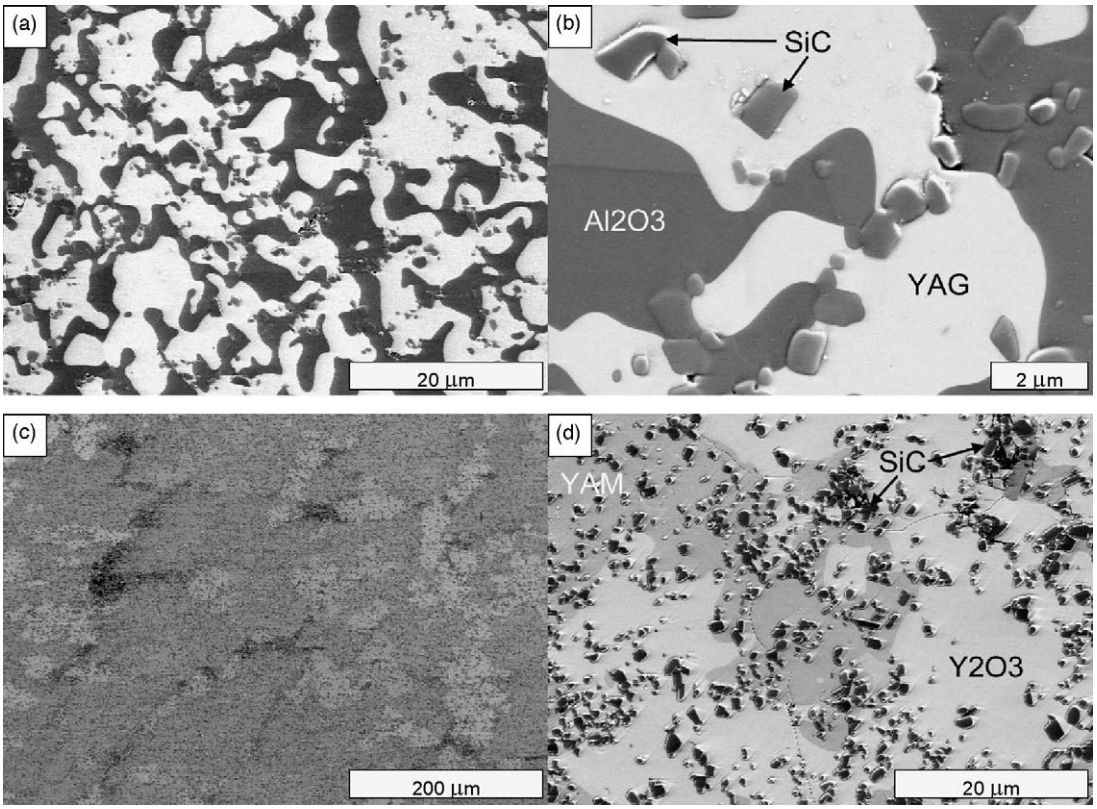

Fig. 5. FESEM micrograph (SE-mode) of YAlSiC-208010 (a and b) and YAlSiC-802050 (c and d) after heat treatment in graphite furnace at 1850 °C (YAlSiC-208010) and 1950 °C (YAlSiC-802050).

Table 3
Melting and crystallisation temperatures and phases identified by XRD measurements for the samples after STA-measurement. Melting temperatures according to thermodynamical calculations (YAG – $Al_5Y_3O_{12}$, YAP – $AlYO_3$, YAM – $Al_2Y_4O_9$).

Sample	[°C]			Phase identification					
	$T_{melting}$	$T_{solidification}$	$T_{melting\ calc.}$	SiC	Al_2O_3	YAG	YAP	YAM	Y_2O_3
YAlSiC-									
208000	1825	1815	1806						
208010	1819	1796	1800	x	x	x			
208020	1817	1798	1796	x	x	x			
YAlSiC-									
455500	1917	1915	1903						
455510	1910	1809	1842	x	x		x		
455520	1911	1826	1842	x	x		x		
YAlSiC-									
604000	1914	1858	1912						
604010	1919	1895	1845	x			x	x	
604020	1920	1893	1845	x			x	x	
YAlSiC-									
802000	1972	1968	1950						
802010	1968	1950	1893	x				x	x
802050	n/a	n/a	1893	x				x	x

The endothermal peak in the DTA-signal at 1819 °C indicates the melting of the additive phases. This is also shown in Fig. 4, which gives a more detailed view on the DTA effects of YAlSiC-208010 and YAlSiC-208020 from 1700 °C to 1850 °C. The fact that the additive phases were molten is confirmed by SEM analysis of the sample treated in the graphite heated furnace which shows undissolved SiC grains in a eutectic matrix of the additive phases YAG and Al_2O_3 (Fig. 5). Solidification is indicated by the exothermal peak at cooling and begins at 1796 °C.

With melting a simultaneous mass loss occurs which finishes when solidification begins. An explanation for this mass loss can be that the phase reactions between SiC and the oxide additives are accelerated in liquid. One of the possible phase reactions are reactions between SiC and Al_2O_3 forming volatile gas species Al_2O, CO and SiO.[8,19] Additionally some interactions with the crucible might take place.

The exothermal decline in the DTA-signal from 1600 °C to 1780 °C is only observed in SiC containing samples (Fig. 4). The higher the SiC content is, the more pronounced the decline is. Samples without SiC do not show this effect.

The determined melting and solidification temperatures and the phases identified by XRD after the STA-measurement of all samples are summarised in Table 3. Additionally the melting temperatures experimentally determined in present study are compared with results of thermodynamic calculations and literature values in Fig. 6.

Regarding the samples with the same yttria–alumina ratio, samples without SiC have higher melting temperatures than the ones without. The sample group YAlSiC-6040x is an exception and the differences are close to the relative uncertainty of measurement. But the tendency over all sample groups is apparent. Thus definite influence of the SiC content on the melting temperature can be concluded. This corresponds to the assumed low solubility (<10%, [10]) of SiC in the oxide melt, since the dissolution of SiC would lower the melting temperature. Both experiments and calculations show that samples with the same yttria–alumina ratio and SiC contents of 10 mol% and 20 mol%, respectively, do not differ significantly in melting temperatures.

Samples YAlSiC-455510 and YAlSiC-455520 show remarkable differences (101 K and 85 K, respectively) in the experimentally determined melting and solidification temperatures (Table 3). Reason for this can be super-cooling of melt.

For the sample YAlSiC-802050 with a high SiC content in comparison to the other samples melting temperatures could not be measured because a mass loss occurred already at 1690 °C without DTA-effect characteristic for melting. The reason for this mass loss can be an accelerated decomposition of SiC due to a high amount of SiC surface.

Optimisation of thermodynamic parameters in the Y_2O_3–Al_2O_3 system based on all available phase equilibrium data and thermodynamic values was performed by Fabrichnaya et al.[12] and up-dated by Fabrichnaya et al.[20] The uncertainty in comparison with experimental values for temperature of eutectic reactions and congruent melting of compounds reaches ±40 °C. Experimental data obtained in

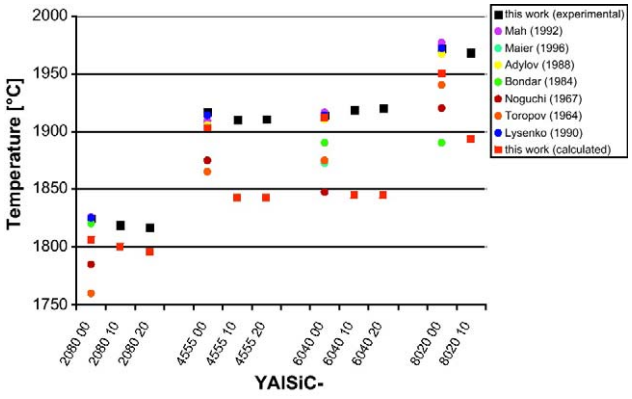

Fig. 6. Comparison of melting temperatures determined in this work with literature data. Values of Lysenko and Voronin[23] are from thermodynamical calculations. The others are experimentally determined.

Table 4
Phases identified by XRD measurements after melting of samples in graphite furnace (YAG – $Al_5Y_3O_{12}$, YAP – $AlYO_3$, YAM – $Al_2Y_4O_9$).

Sample	T_{max}	Phase identification					
	[°C]	SiC	α-Al_2O_3	YAG	YAP	YAM	Y_2O_3
YAlSiC-							
208010	1850	x	x	x			
208020	1850	x	x	x			
YAlSiC-							
455510	1950	x		x	x		
455520	1950	x		x	x		
YAlSiC-							
604010	1950	x			x	x	
604020	1950	x			x	x	
YAlSiC-							
802050	1950	x				x	x

present study for Al_2O_3–Y_2O_3 system are in good agreement with experimental results of Mah and Petry[21] and Adylov et al.[22], with calculations of Lysenko and Voronin[23] and Fabrichnaya et al.[20] The comparison of experimental data with thermodynamic calculations for samples containing SiC indicates that temperatures of melting for samples 4555x, 6040x and 8020x are up to 75 °C lower in calculations. This difference can only be explained by the fact that according to calculations SiC decomposes forming SiO_2 which dissolves in the liquid and decreases melting temperature. It should be mentioned that the solubility of SiC in the melt has not been modelled yet.

Phases identified in samples by XRD after the STA-measurements and in samples heat treated in the graphite furnace are summarised in Tables 3 and 4, respectively. All samples treated in the graphite furnace were molten after the heat treatment, and all of them consisted of SiC and the phases expected from the pseudo binary system Al_2O_3–Y_2O_3 (see Table 2). The phase assemblages obtained by thermodynamic calculations of the ternary system SiC–Al_2O_3–Y_2O_3 are the same as identified experimentally except for very small amount of Al_4SiC_4 found by calculations for mixtures with high Y_2O_3 content. Additionally reactions of carbide or oxycarbide formation took place at the interface between graphite and melt.

For the samples examined in the STA the situation is different. The YAlSiC-2080x samples show the equilibrium phases after heat treatment, whereas the YAlSiC-4555x samples showed YAP and alumina, which are not equilibrium phases according to phase diagram. An explanation could be the formation of a metastable eutectic of Al_2O_3 and YAP mentioned by Caslavsky and Viechnicki.[24] The SiC content was difficult to determine. This is because of the partial overlapping of the SiC reflections with the other phases occurs.

Samples were additionally analysed by SEM and EDX after heat treatment in the graphite furnace. Fig. 5 shows, as an example, the micro-structure of YAlSiC-208010 (a and b) and YAlSiC-802050 (c and d) in SE-mode in different magnifications. The eutectic structures, once Al_2O_3 and YAG and once Y_2O_3 and YAM with fine distributed and partially agglomerated, small SiC grains were observed. This confirms the assumption of a low solubility of SiC in the oxide melt which has already been shown through the decrease in the melting temperatures.

4. Conclusions

Melting temperatures in the system SiC–Al_2O_3–Y_2O_3 were determined using STA-measurements. The results for samples of the boundary system Al_2O_3–Y_2O_3 are in good agreement with literature data and calculations. The new results for the ternary system show a small influence of the SiC content on the melting temperatures. This confirms the assumption of a low solubility of SiC in the oxide melt. Also the SEM analysis, where fine distributed SiC grains in a eutectic matrix can be observed, supports this statement.

The phase formation in the system follows the statement that SiC and the aluminates are in equilibrium.

Acknowledgement

The authors would like to thank the German Research Foundation for financial support (HE 2457/14-1 and SE 647/10-1).

References

1. Böcker WDG. In: Kollenberg W, editor. *Technische Keramik Grundlagen Werkstoffe Verfahrenstechnik*. Essen: Vulkan-Verlag; 2004.
2. Schwetz KA. Silicon carbide based hard materials. In: Riedel R, editor. *Handbook of ceramic hard materials*. Weinheim: Wiley-VCH; 2002. p. 683–748.
3. Gubernat A, Stobierski L, Labaj P. Microstructure and mechanical properties of silicon carbide pressureless sintered with oxide additives. *J Eur Ceram Soc* 2007;**27**(2–3):781–9.
4. Omori M, Takei H. Pressureless sintering of SiC. *J Am Ceram Soc* 1982;**65**:C92.
5. Volz E, Roosen A, Hartung W, Winnacker A. Electrical and thermal conductivity of liquid phase sintered SiC. *J Eur Ceram Soc* 2001;**21**:2089–93.
6. Herrmann M, Schilm J, Michael G. Corrosion behaviour of different technical ceramics in acids, basic solutions and under hydrothermal condition. *Ceram Forum Int* 2003;**80**(4):E27–33.
7. Baud S, Thévenot F, Pisch A, Chatillon C. High temperature sintering of SiC with oxide additives. I. Analysis in the SiC–Al_2O_3 and SiC–Al_2O_3–Y_2O_3 systems. *J Eur Ceram Soc* 2003;**23**:1–8.
8. Ihle J, Herrmann M, Adler J. Phase formation in porous liquid phase sintered silicon carbide. Part III. Interaction between Al_2O_3–Y_2O_3 and SiC. *J Eur Ceram Soc* 2005;**25**:1005–13.
9. Cupid DM, Fabrichnaya O, Seifert HJ. Thermodynamic aspects of liquid phase sintering of SiC using Al_2O_3 and Y_2O_3. *Int J Mater Res* 2007;**98**:976–86.
10. Hoffmann MJ, Nader M. In situ toughening of non oxide ceramic-opportunities and limits. In: Babini GN, Haviar M, Šajgalík P, editors. *Engineering ceramics ĭ96: higher reliability through processing 3. High technology*, vol. 25. Dordrecht, Boston, London: Kluwer Academic Publishers; 1997.
11. Pan Z, Fabrichnaya O, Seifert HJ, Neher R, Brandt K, Herrmann M. Thermodynamic evaluation of the Si–C–Al–Y–O System for LPS-SiC Application. *J Phase Equilib Diffus* 2010, doi:10.1007/s11669-010-9695-7.
12. Fabrichnaya O, Seifert HJ, Weiland R, Ludwig T, Aldinger F, Navrotsky A. Phase equilibria and thermodynamics in the Y_2O_3–Al_2O_3–SiO_2 system. *Zeitschrift für Metallkunde* 2001;**92**:1083–97.
13. Gröbner J. Konstitutionsberechnungen in system Y–Al–Si–C–O. PhD Thesis. University of Stuttgart, Germany; 1994.
14. Andersson JO, Helander T, Höglund L, Shi P, Sundman B. Thermo-calc & DICTRA, computational tools for material science. *CAlPHAD* 2002;**26**:273–312.

15. Omori M, Takei H. Preparation of pressureless-sintered SiC–Y_2O_3–Al_2O_3. *J Mater Sci* 1988;**23**.
16. Sciti D, Bellosi A. Effects of additives on densification, microstructure and properties of liquid-phase sintered silicon carbide. *J Mater Sci* 2000:35.
17. Taguchi SP, Motta FV, Balestra RM, Ribeiro S. Wetting behaviour of SiC ceramics. Part II – Y_2O_3/Al_2O_3 and Sm_2O_3/Al_2O_3. *Mater Lett* 2004:58.
18. Zhang N, Rub HQ, Cai QK, Sunb XD. The influence of the molar ratio of Al_2O_3 to Y_2O_3 on sintering behaviour and the mechanical properties of a SiC–Al_2O_3–Y_2O_3 ceramic composite. *Mater Sci Eng A* 2008:486.
19. Mulla MA, Krstic VD, Thompson WT. Reaction-inhibition during sintering of SiC with Al_2O_3 additions. *Can Metall Quart* 1995;**34**(4):357–62.
20. Fabrichnaya O, Zinkevich M, Aldinger F. Thermodynamic modelling in the ZrO_2–La_2O_3–Y_2O_3–Al_2O_3 system. *Int J Mater Res* 2007;**98**(9):838–46.
21. Mah T, Petry MD. Eutectic composition in the pseudobinary of $Y_4Al_2O_9$ and Y_2O_3. *J Am Ceram Soc* 1992;**75**(7):2006–9.
22. Adylov GT, Voronov GV, Mansurova EP, Sigalov LM, Urazaeya EM. System Y_2O_3–Al_2O_3, figure 09265. In: *ACerS-NIST, phase equilibria diagrams, CD-ROM database, version 3.1, National Institute of Standards and Technology Standard Reference Database 31*. 1988.
23. Lysenko VA, Voronin GF. System Al_2O_3–Y_2O_3. Calculated, temperature-composition melting equilibria, figure 11119. In: *ACerS-NIST, phase equilibria diagrams, CD-ROM database, version 3.1, National Institute of Standards and Technology Standard Reference Database 31*. 1990.
24. Caslavsky JL, Viechnicki DJ. Melting behaviour and metastability of yttrium aluminium garnet (YAG) and $YAlO_3$ determined by optical differential thermal analysis. *J Mater Sci* 1980;**15**:1709–918.